NATIONAL ADVISORY COMMITTEE
FOR AERONAUTICS

TECHNICAL NOTE 4351

SUMMARY OF METHODS OF MEASURING

ANGLE OF ATTACK ON AIRCRAFT

By William Gracey

Langley Aeronautical Laboratory
Langley Field, Va.

NACA

E

NATIONAL ADVISORY COMMITTEE FOR AERONAUTICS

TECHNICAL NOTE 4351

SUMMARY OF METHODS OF MEASURING

ANGLE OF ATTACK ON AIRCRAFT

By William Gracey

SUMMARY

Wind-tunnel calibrations of three types of angle-of-attack sensing devices - the pivoted vane, the differential pressure tube, and the null-seeking pressure tube - are presented. The pivoted vane has been used primarily in the flight testing of airplanes and missiles, whereas the null-seeking pressure tube has been used almost exclusively in the service operation of airplanes. The differential pressure tube has not been used to any great extent as a flight instrument.

Flight data on the position errors for three sensor locations - ahead of the fuselage nose, ahead of the wing tip, and on the forebody of the fuselage - are also presented. For operation throughout the subsonic, transonic, and supersonic speed ranges, a position ahead of the fuselage nose will provide the best installation. If the shape of the fuselage nose is not too blunt, the position error will be essentially zero when the sensor is located 1.5 or more fuselage diameters ahead of the fuselage.

Various methods for calibrating angle-of-attack installations in flight are briefly described.

INTRODUCTION

Angle of attack is defined as the angle between the relative wind in the plane of symmetry and the longitudinal axis of the airplane. The measurement of this quantity has received increasing attention in recent years because of its requirement for fire control, cruise control, and stall warning.

Sensing devices for measuring angle of attack may be located either ahead of the aircraft (usually on booms mounted on the wing tip or the

fuselage nose) or on some part of the aircraft itself. For any position
on or near the aircraft, however, the sensing device will measure the
local rather than the true angle of attack. The amount by which the
local angle of attack differs from the true angle of attack is called
the position error of the installation. This error varies with the lift
coefficient and Mach number of the aircraft. For some locations of the
sensing device, the position error may also vary with changes in the con-
figuration of the aircraft, for example, flap deflection, landing-gear
extension, and so forth.

The overall error of an installation includes errors peculiar to
the sensing device in addition to the errors due to the location of the
device. The errors of the sensing device are generally determined by
wind-tunnel tests. The position error, on the other hand, must be deter-
mined by calibration of the installation in flight. In accelerated
maneuvers, additional errors may be introduced by such items as the
pitching velocity of the aircraft, boom bending, fuselage flexibility,
and lag in the transmission system of the angle-of-attack instrumentation.

A description of various types of angle-of-attack devices and their
application to stall warning is presented in reference 1. A comprehen-
sive survey of possible types of instrumentation for the measurement of
angle of attack on aircraft is given in reference 2. In a similar study
(ref. 3) a method is developed for determining angles of attack and side-
slip from measurements of the motions of the aircraft.

The present report summarizes experimental data on sensing devices
which have found practical application in the testing of airplanes and
missiles or which have been test evaluated for possible use on aircraft.
The position errors of several types of installation and some flight
calibration methods for determining these errors are also presented.

SYMBOLS

α angle of attack (angle between relative wind in the plane of
symmetry and the longitudinal axis of the airplane), deg

α_l local angle of attack, deg

$\Delta\alpha$ angle-of-attack error $(\alpha_l - \alpha)$, deg

β angle of sideslip, deg

Δp pressure difference between orifices on differential pressure
tube

q   dynamic pressure

M   Mach number

C_N normal-force coefficient

c   local wing chord

D   maximum effective fuselage diameter

x   distance of sensor ahead of wing or fuselage

l cone length (conical differential pressure tube)

SENSING DEVICES

The types of sensing devices which have been used for the measurement of angle of attack are the pivoted vane, the differential-pressure tube, and the null-seeking pressure tube. The pivoted vane has been used primarily in the flight testing of airplanes and missiles, whereas the null-seeking pressure tube has been used almost exclusively in the service operation of airplanes. The differential pressure tube has not been used to any great extent as a flight instrument.

Pivoted Vanes

A pivoted vane is a mass-balanced wind vane free to aline itself with the direction of the air flow. The vane may be mounted either ahead of a boom support or on a transverse shaft which is attached to a boom or to the body of the airplane. The angles measured by a vane mounted on a boom will be influenced by (1) distortion of the flow when the boom is inclined to the flow (upwash effect), (2) asymmetry of the vane due to imperfections in manufacture (floating angle), and (3) bending of the boom support due to air loads.

In maneuvering flight, additional errors may be introduced because of further bending of the boom (as a result of normal and pitching accelerations) and the pitching velocity of the airplane. In the case of a flexible airplane, consideration may also have to be given to the effects of flexibility of the structure.

The magnitude of the upwash effect of both axially and transverse-mounted vanes depends on the diameter of the boom support. For a vane on a transverse shaft, the magnitude of the effect also depends upon the

distance of the vane from the axis of the boom. In this case the effect
of upwash may be minimized by locating the vane at least two boom diame-
ters from the boom axis (ref. 4).

Corrections for upwash around the boom may be determined by cali-
brating the sensing device in a wind tunnel. The floating angle of the
vane can be determined at the same time by calibrating the device in
upright and inverted positions. The floating angle is determined as
one-half the difference between indications in the two positions. As
noted in reference 4, the floating angle may also be determined in flight
by calibrating the vane in upright and inverted positions on successive
flights. In this method a second angle-of-attack system is required as
a reference for the vane measurements.

As noted previously, bending of the boom may occur as a result of
aircraft air loads and aircraft acceleration. Deflection of the boom
due to air loads may be estimated from information on drag coefficients
of cylinders or may be computed from wind-tunnel measurements of the
particular boom being used. Boom deflections due to normal and pitching
accelerations may be computed from the recorded values of the aircraft
accelerations and from ground calibrations of the boom deflection as
obtained by applying various weights to the boom. A more direct measure
of the deflection due to both air loads and accelerations is one in which
the boom is photographed in flight with a camera installed in the fuse-
lage of the airplane. A detailed discussion of the methods of determining
upwash effect, floating angle, and boom bending is given in reference 4.

Axially mounted pivoted vanes.- A pivoted vane designed for mounting
ahead of a boom support is described in reference 5. As shown by the
diagram on figure 1(a), the sensor consists of a conical body with a
triangular vane attached to the rear portion of the cone. This sensor
was developed for the testing of missiles and is, for this reason, com-
paratively small. The length of the conical body is $3\frac{1}{4}$ inches and the
span of the vane about $2\frac{3}{4}$ inches. The shaft to which the vane is con-
nected is designed for attachment to a $\frac{3}{4}$-inch-diameter boom.

The vane unit has a maximum range of $\pm15^\circ$. The results of wind-
tunnel tests (ref. 5) for an angle-of-attack range of -4° to 12° ($\beta = 0^\circ$)
are presented in figure 1(b). The data were obtained at Mach numbers of
0.85, 0.95, and 1.20. The large scatter of the test points at M = 0.85
and 0.95 is believed to be due to friction or play in the transmitting
linkage and sliding-core pickup.

Transverse-mounted pivoted vanes.- A type of pivoted vane in which
the vane is mounted on a shaft attached to the side of the boom support

is shown in figure 2(a). The sensing device shown in this figure incorporates two vanes oriented 90° apart. In addition to measurements of angles of attack and sideslip, this instrument also measures pitot and static pressures. This sensing device was especially developed for the flight testing of research aircraft and is designed for mounting on a fuselage-nose boom.

The results of a wind-tunnel calibration (ref. 6) of the angle-of-attack vane at M = 0.6 to 1.10 are presented in figure 2(b). The vane was calibrated over an angular range of -5° to 25°. The slopes of the curves are a measure of the upwash around the boom. The errors at α = 0 would appear to be an indication of the floating angle of the vane.

Wind-tunnel tests of another instrument of this type at higher Mach numbers (1.61 to 2.01) are reported in reference 7. The results of these tests which covered an angle-of-attack range of -3° to 20° at M = 1.61 and -3° to 24° at M = 2.01 are presented in figure 2(c). In these tests, three vanes were tested to check any variations due to manufacturer. The results showed no significant differences in the floating angles of the three vanes.

Differential-Pressure Tube

An angle-of-attack sensor of the differential-pressure-tube type consists of two orifices oriented at equal angles on either side of the longitudinal axis of the tube. The pressure difference which exists at the two orifices when the tube is inclined to the flow is a measure of the angle of attack of the tube. At any given angle of attack the magnitude of this pressure difference depends principally on the shape of the nose of the tube, on the angular position of the orifices, and to some extent on Mach number and Reynolds number.

The two types of nose shape which have been used to the greatest extent in the design of differential-pressure sensors are the hemisphere and the cone. For these shapes the greatest sensitivity of the tube to angle of attack can be achieved by orientating the orifices about 90° apart on the hemisphere (see data in ref. 8) or, in the case of the cone, by using a 90° cone angle.

As the angle of attack of a differential pressure sensor is a function of the ratio of the pressure difference to the impact pressure, the use of this type of tube requires the measurement of two quantities. If recording instruments are used, the two quantities can be recorded separately and the angle of attack determined by computation. If, however,

a direct indication of the angle of attack is desired, a pressure-ratio
type of instrument must be employed.

Data from wind-tunnel tests of differential-pressure sensors having
hemispherical nose shapes are presented in figures 3 and 4. The sensor
shown in figure 3(a) was about $1\frac{1}{4}$ inches in diameter with two orifices
spaced 90° apart. The data for this sensor were from a report of limited
availability by G. F. Moss and N. K. Walker of the British Royal Aircraft
Establishment. The tests were conducted at a Mach number of about 0.11
through an angle-of-attack range of $\pm 20^{\circ}$. The variation of $\Delta p/q$ with
α for these test conditions is given in figure 3(b). The two sensors
shown in figure 4(a) were 1/2 inch in diameter and were tested by the
Engineering Physics Department at Cornell Aeronautical Laboratory, Inc.
The orifices of one of the tubes were spaced 60° apart and those of the
other, 90° apart. The tests covered a range of Mach number of 0.3 to
0.8 and an angular range of 0° to 20°. Sample results of the tests at
$M = 0.35$ and 0.60 are presented in figure 4(b). These data show that
the tube with the orifices spaced 90° apart is more sensitive to angle
of attack than the tube with orifices spaced 60° apart. The data also
show the sensitivity of both tubes to decrease as the Mach number
increases. A comparison of the data in figures 3 and 4 shows the sensi-
tivity of tube A in figure 4 to be greater than that of the tube shown
in figure 3 despite the fact that the orifices on both of the tubes are
spaced 90° apart. The Mach number trend shown in figure 4 does not
account for this difference and no other explanation for the difference
can be found in the reports of these two tests.

The use of conical nose shapes for measurements at supersonic speeds
has received considerable attention because the measurement of total pres-
sure at the nose of the cone, in combination with the pressures on the
surface of the cone, can provide indications of Mach number and static
pressure as well as angles of attack and sideslip. Wind-tunnel tests to
determine the accuracy with which Mach number and angle of attack can be
calculated from the pressures on a 15° cone at $M = 1.59$ are reported
in reference 9.

Wind-tunnel data of conical-nosed tubes having apex angles of 30°,
40°, and 50° were also made at the Cornell Aeronautical Laboratory, Inc.
The body diameter of each tube was 1/2 inch and the orifices on each of
the tubes were located 2/3 of the cone length behind the apex. (See
fig. 5(a).) The tests were conducted at $M = 0.30$ to 0.65 through an
angle-of-attack range of 0° to 20°. Sample calibrations of the tubes
at $M = 0.35$ and 0.60 are presented in figure 5(b). These curves show
the sensitivity of the tubes to decrease as the apex angle decreases.
For the range of Mach numbers covered by the tests, the effect of Mach
number on the sensitivity is small for the 50° probe and negligible for
the 30° and 40° probes.

Calibrations at transonic speeds of a conical-nosed sensor having
an apex angle of 45° were performed by the wing-flow method. (See
ref. 10.) The tube was 1 inch in diameter and the orifices were located
0.674 inch from the nose. (See fig. 6(a).) The tests were conducted at
$M = 0.70$ to 1.10 through an angular range of -10° to 50°. A single
curve, representing the mean of the test data obtained throughout the
test range is presented in figure 6(b). Although the scatter of the
test points as presented in reference 10 was as much as 1.5° at some
angles of attack, there was no consistent variation of $\Delta p/q$ with Mach
number. This scatter of the test data and the fact that the curve does
not pass through the origin was noted in reference 10 as being the
result of play in the actuating mechanism used to rotate the tube through
the angle-of-attack range.

Supersonic wind-tunnel tests of a conical-nosed sensor having a 20°
apex angle are reported in reference 11. The body of the sensor was
3/8 inch in diameter with orifices located 1/4 inch from the apex. (See
fig. 7(a).) The tests were conducted at $M = 1.5, 1.6$, and 1.7 through
a range of angle of attack of -5° to 10°. The results of the tests are
presented in figure 7(b). No explanation is given in reference 11 for
the fact that the curves for $M = 1.5$ and 1.6 do not pass through the
origin.

Null-Seeking Pressure Sensor

A null-seeking pressure sensor for measuring angle of attack con-
sists of (1) a rotatable tube with two orifices disposed at equal angles
to the axis of the tube, (2) a pressure-sensitive device for detecting
the pressure difference between the two orifices when the tube is inclined
to the flow, (3) a mechanism for rotating the tube to the null-pressure
position, and (4) instrumentation for measuring the angular position of
the tube. The advantages of this tube as compared with the differential-
pressure tube are (1) the measurements are independent of impact pressure,
Mach number, and Reynolds number and (2) the differential-pressure sensing
elements can be comparatively sensitive because the operating differential
pressures should be always near zero, provided of course, the response of
the system is sufficiently rapid.

An example of a sensing device of the null-seeking pressure-tube
type is illustrated in figure 8(a). This device consists of a rotatable
cylindrical tube which protrudes through the wall of the fuselage and an
air chamber system which is housed inside the fuselage. The tube is
3/8 inch in diameter and about $3\frac{3}{8}$ inches long and incorporates a pair of
slots spaced 60° apart. The interior of the tube is divided into two
sections which vent to a pair of air chambers formed by a swivel paddle

vane. A pressure difference at the two slots causes rotation of the
paddle vane which, by means of a linkage, rotates the pressure tube
until the pressures are equalized. The angular position of the probe
is then measured by a potentiometer.

Wind-tunnel tests of this device at 75 to 125 miles per hour are
reported in reference 12. The instrument was calibrated over an angular
range of -15° to 14°. Sample results of the tests are presented in
figure 8(b) for a speed of 75 miles per hour (M = 0.10). As shown by
this figure the mean error was within ±0.1° over the angular range of
the tests. The scatter of the test points about the mean curve was
within about ±0.2°. Dynamic-response tests indicated that at frequencies
between 0.8 and 1.8 cps the amplitude frequency response was about 90 per-
cent at 100 miles per hour and 97 percent at 150 miles per hour.

Another type of null-seeking pressure tube (fig. 9(a)), designed
for mounting on the end of a horizontal boom, is described in reference 8.
The sensing element of this device consists of an ellipsoidal nose tube,
2 inches in diameter, with two orifices oriented at equal angles with
respect to the longitudinal axis of the tube. The orifices are connected
to a sensitive pressure capsule located in the nose of the tube. Deflec-
tion of the capsule produces a signal which operates a servomechanism
which, in turn, rotates the tube to the null-pressure position. The
position of the tube is then measured by a synchro-system.

The results of low-speed wind-tunnel tests of this device are pre-
sented in figure 9(b). The error, which is caused by the upwash
around the boom, varies from -1° at an angle of attack of -10° to 1.2°
at an angle of attack of 12°. The accuracy of the measurements is ±0.1°.
Dynamic-response tests indicated that, with the type of servomechanism
used with this tube, the amplitude frequency response is close to 100 per-
cent up to 1.3 cycles per second.

POSITION ERRORS

Because of the flow field created by the aircraft, the flow angle
at any given location in the vicinity of the aircraft will generally
differ from the true angle of attack of the aircraft. At subsonic speeds
the effects of the flow field extend in all directions from the aircraft.
At supersonic speeds the effects are confined to regions behind the shock
waves which form ahead of the aircraft. Thus, angle-of-attack sensors
located ahead of the foremost airplane shock should be unaffected by the
flow field of the aircraft at supersonic speeds.

As the flow field around each aircraft configuration is unique, the position error (that is, the difference between local and true angles of attack) at a given location with respect to the aircraft will vary from one aircraft to another. Exact values of the position errors of a given installation on a specific aircraft, therefore, can be determined only by calibration of the installation in flight. Flight calibrations of installations on specific airplanes, however, can provide an indication of relative magnitudes and trends of the position errors for given locations of the sensing device. Three sensor positions which have proved successful and which have been used to the greatest extent are positions ahead of the fuselage nose, ahead of the wing tip, and on the forebody of the fuselage.

Positions Ahead of Fuselage Nose

At speeds below the Mach number at which the fuselage bow shock passes the angle-of-attack sensor, the position error at a given distance ahead of the fuselage depends on the maximum diameter of the fuselage and the shape of the fuselage nose section.

The variation of local angle of attack with distance ahead of a fuselage having a rounded ogival nose shape is presented in figure 10 for a constant Mach number of 0.80 (unpublished data obtained at the Ames Aeronautical Laboratory). The data in this figure show that for each value of normal-force coefficient the local angle of attack decreases (and approaches the true angle of attack) as the distance from the nose increases.

The variation of local angle of attack with distance ahead of the nose of a fuselage having a nose inlet is presented in figure 11 for a constant Mach number of 0.81. (See ref. 13.) The flow-angle variation of this installation is similar to that for positions ahead of the fuselage having a rounded ogival nose shape. The data from the two airplanes indicate that, for fuselage nose shapes no blunter than these, the local angle of attack will be very nearly the true angle of attack at positions 1.5 or more fuselage diameters ahead of the fuselage nose. Because an angle-of-attack sensor located ahead of the nose will come under the influence of only one shock (the fuselage bow wave), sensor locations ahead of the fuselage nose are considered to be preferable to wing tip and fuselage surface positions, particularly for transonic and supersonic operation.

Positions Ahead of Wing Tip

Prior to the passage of the wing and fuselage bow shocks over the sensor, the position error at a given distance ahead of the wing of an

airplane is determined by the maximum thickness of the local airfoil,
the shape of the airfoil section, the sweepback angle of the wing, and
the spanwise location. At the Mach numbers at which the wing and fuse-
lage bow shocks pass or are in the vicinity of the sensor, large errors
may be introduced due to variations of angle of sideslip.

At subsonic speeds the position error varies with distance ahead of
the wing in a manner similar to that for positions ahead of the fuselage
nose. Because of the lifting characteristic of the wing, however, the
position errors of wing-tip installations are apt to be larger than
those of comparable fuselage-nose installations. A calibration of a
differential-pressure type angle-of-attack sensor located 0.5 chord
length ahead of the wing tip of an airplane is presented in figure 12
(data from Cornell Aero. Lab., Inc., for M = 0.3).

Positions on the Surface of the Fuselage Nose

Calibrations of an angle-of-attack sensor on the surface of the
fuselage nose of an airplane were determined from tests reported in
reference 13. The sensor was a null-seeking pressure type and was
located near the center line of the fuselage and about midway from the
nose to the leading edge of the wing. The local angle of attack indi-
cated by the sensor was compared with the angle of attack measured by a
vane-type sensor located about $1\frac{2}{3}$ fuselage diameters ahead of the fuse-
lage nose. The measurements from the vane were considered to represent
the true angles of attack of the airplane.

The tests were conducted over a Mach number range of 0.6 to 1.02.
Sample calibrations of the installation at M = 0.6, 0.81, and 0.92
are given in figure 13. These data, as well as those at the other test
speeds, show a linear variation of local angle of attack with true angle
of attack. The data also show that for constant angle of attack the
local angle of attack decreases as the Mach number increases. In addi-
tion, the local angle of attack is shown to change about 1.6° for each
degree change in true angle of attack. For other locations of the sensor
on the nose and for other fuselage nose shapes, the variations of local
angle of attack with true angle of attack will, of course, be different.

The effect of angle of sideslip on the angle of attack indicated
by the sensor was determined at constant true angles of attack at
M = 0.70 to 0.91. As shown by the curves in figure 14, the variation
of indicated angle of attack with sideslip was linear and amounted to
0.1° angle of attack for each degree of sideslip. These data also indi-
cate that for small sideslip angles the effect of sideslip can be elimi-
nated by installing sensors on each side of the fuselage and averaging
the two indications.

FLIGHT CALIBRATION METHODS

An angle-of-attack installation may be calibrated in flight by any one of a number of methods. Some of the methods are applicable only to unaccelerated flight, whereas others may be employed for maneuvering flight as well. As the instrumentation and procedure for some of the methods are very involved, only a general description of the methods will be given here.

Attitude-Angle Method

In level unaccelerated flight and in the absence of vertical air currents, the attitude angle of an airplane is equal to its angle of attack. In localities where the horizon is not obscured by haze, the attitude angle can be measured easily by photographing the horizon from a camera installed in the airplane and directed either forward or to the side. For a camera directed forward, corrections must be applied for the curvature of the earth. (See ref. 14.)

In those cases where it is impractical to photograph the horizon, the attitude angle of the airplane may be determined by photographing the sun. The elevation angle of the sun is determined from the longitude and latitude of the airplane, from navigation tables, and from a precise measure of time. (See ref. 15.)

The attitude angle of the aircraft may also be measured with a pendulum inclinometer. (See ref. 16.) The angles measured by this instrument, however, are subject to errors due to variations in longitudinal acceleration. For this reason, the use of an inclinometer will generally prove more unsatisfactory than the use of horizon or sun cameras, both of which are unaffected by aircraft acceleration.

The greatest difficulty in applying the attitude-angle method is encountered in attempting to maintain level flight. Standard aircraft altimeters are not sufficiently sensitive to provide the high order of accuracy usually required. For this reason, a sensitive recording statoscope should be used for detecting deviations from constant altitude. If appreciable changes in altitude occur during the tests, the attitude—flight-path-angle method described in the next section should be applied.

Another difficulty in the application of the attitude angle method involves the effect of vertical air currents. Best results would appear to be obtained by conducting the tests at low altitudes (preferably over

a large body of water) because the magnitude of the vertical air currents would be expected to be smaller than at higher altitudes.

Attitude—Flight-Path Angle Method

A method by which an installation can be calibrated when the airplane is changing altitude involves the measurement of flight-path angle in conjunction with the attitude angle. The flight-path angle is determined from simultaneous measurements of the vertical velocity and the velocity along the flight path.

The vertical velocity may be measured with a recording statoscope or by integrating a time history of the vertical acceleration, which may be calculated from the recorded normal and longitudinal accelerations and the attitude angle.

As discussed in the previous section, the attitude angle may be measured with a horizon camera or a sun camera. In some cases it may be more convenient to measure only the initial attitude angle with a sun camera, horizon camera, or inclinometer and then to determine the change in attitude angle from measurements with an attitude gyroscope or from integration of the recorded pitching velocity.

The calculation of angle of attack by the attitude—flight-path angle method requires that the records of each of the measured quantities have a time scale and a means of synchronization.

Fuselage-Nose-Boom Method

In the fuselage-nose-boom method the local angle of attack at a point a considerable distance ahead of the fuselage is considered to represent a close approximation to the true angle of attack of the airplane. The angle-of-attack measurement is most conveniently made by means of a pivoted vane installed on a boom extending ahead of the fuselage nose. Tests to determine the variation of local angle of attack with distance ahead of the fuselages of an airplane (ref. 13) showed that, with increasing distance ahead of the fuselage, the local angle of attack approached the true angle of attack asymptotically and that at a distance of at least 1.5 fuselage diameters the local angle of attack was essentially equal to the true angle of attack. Calibrations in which this method was employed in tests on another airplane are reported in reference 17. When the tests are conducted in accelerated flight, corrections must, of course, be applied for bending of the boom, pitching velocity of the airplane, and bending of the fuselage.

Ground Photographic Methods

A method has been developed in which the angle of attack is determined from the flight-path angle as determined from a camera on the ground and the attitude angle as measured by a camera installed in the airplane. The direction and velocity of the wind are determined from photographs by the ground camera of smoke puffs released from the airplane. The method was developed for the special case of an airplane diving toward a ground target at a predetermined dive angle. As described in references 18 and 19, the method requires that the ground camera be located at the center of the target and elevated to the proposed dive angle of the airplane. The camera in the airplane photographs the ground target during the dive. An extension of this method to permit calibration during the pull-up following the dive required the use of two ground cameras and three surveyed ground markers. (See ref. 20.)

CONCLUDING REMARKS

Wind-tunnel calibrations of three types of angle-of-attack sensing devices - the pivoted vane, the differential pressure tube, and the null-seeking pressure tube - have been presented. The pivoted vane has been used primarily in the flight testing of airplanes and missiles, whereas the null-seeking pressure tube has been used almost exclusively in the service operation of airplanes. The differential pressure tube has not been used to any great extent as a flight instrument.

Flight data on the position errors of three sensor locations - ahead of the fuselage nose, ahead of the wing tip, and on the forebody of the fuselage - have also been presented. For operation throughout the subsonic, transonic, and supersonic speed ranges, a position ahead of the fuselage nose will provide the best installation. If the shape of the fuselage nose is not too blunt, the position error will be essentially zero when the sensor is located 1.5 or more fuselage diameters ahead of the fuselage.

Langley Aeronautical Laboratory,
    National Advisory Committee for Aeronautics,
        Langley Field, Va., March 24, 1958.

REFERENCES

1. Zalovcik, John A.: Summary of Stall-Warning Devices. NACA TN 2676, 1952.

2. Emerson, F. M., Gardner, F. H., Gruenwald, G. D., Olshausen, R., and Sloma, L. V.: Study of Systems for True Angle of Attack Measurement. WADC Tech. Rep. 54-267, U. S. Air Force, May 1955.

3. Smetana, Frederick O., and Stuart, Jay Wm., Jr.: A Study of Angle-of-Attack Angle-of-Sideslip Pitot-Static Probes. WADC Tech. Rep. 57-234, AD 118209, U. S. Air Force, Jan. 1957.

4. McFadden, Norman M., Holden, George R., and Ratcliff, Jack W.: Instrumentation and Calibration Technique for Flight Calibration of Angle-of-Attack Systems on Aircraft. NACA RM A52I23, 1952.

5. Mitchell, Jesse L., and Peck, Robert F.: An NACA Vane-Type Angle-of-Attack Indicator for Use at Subsonic and Supersonic Speeds. NACA TN 3441, 1955. (Supersedes NACA RM L9F28a.)

6. Pearson, Albin O., and Brown, Harold A.: Calibration of a Combined Pitot-Static Tube and Vane-Type Flow Angularity Indicator at Transonic Speeds and at Large Angles of Attack or Yaw. NACA RM L52F24, 1952.

7. Sinclair, Archibald R., and Mace, William D.: Wind-Tunnel Calibration of a Combined Pitot-Static Tube and Vane-Type Flow-Angularity Indicator at Mach Numbers of 1.61 and 2.01. NACA TN 3808, 1956.

8. Young, D. W.: Development of the Null Pressure Type Angle of Attack and Angle of Yaw Indicator. AF Tech. Rep. 6280, ASTIA Doc. Nr. AD 118025, Wright Air Dev. Center, U. S. Air Force, Jan. 1957.

9. Cooper, Morton, and Webster, Robert A.: The Use of an Uncalibrated Cone for Determination of Flow Angles and Mach Numbers at Supersonic Speeds. NACA TN 2190, 1951.

10. McClanahan, Herbert C., Jr.: Wing-Flow Investigation of a 45° Cone as an Angle-of-Attack Measuring Device at Transonic Speeds. NACA RM L51E16, 1951.

11. Davis, Theodore: Development and Calibration of Two Conical Yaw-meters. Meteor Rep. UAC-43, United Aircraft Corp., Oct. 1949.

12. Aircraft Laboratory Aeronautics Division: Specialties Angle of
    Attack Indicator. Memo. Rep. WCNSW 655-1605-1, Wright Air
    Development Center, U. S. Air Force, Mar. 5, 1952.

13. McFadden, Norman M., Rathert, George A., Jr., and Bray, Richard S.:
    Flight Calibration of Angle-of-Attack and Sideslip Detectors on
    the Fuselage of a 35° Swept-Wing Fighter Airplane. NACA RM A52A04,
    1952.

14. Seeley, L. W.: A Simple Technique for the Measurement of Aircraft
    Angle of Attack. NAVORD Rep. 1294 (NOTS 364), U. S. Naval
    Ordnance Test Station, Inyokern (China Lake, Calif.), Mar. 8, 1951.

15. Zalovcik, John A., Lina, Lindsay J., and Trant, James P., Jr.: A
    Method of Calibrating Airspeed Installations on Airplanes at Tran-
    sonic and Supersonic Speeds by the Use of Accelerometer and
    Attitude-Angle Measurements. NACA Rep. 1145, 1953. (Supersedes
    NACA TN 2099 by Zalovcik and NACA TN 2570 by Lina and Trant.)

16. Seeley, Leonard W.: Flight Investigation of a 1-g Angle-of-Attack
    Position-Error Calibration Technique. NAVORD Rep. 2025 (NOTS 681),
    U. S. Naval Ord. Test Station, Inyokern (China Lake, Calif.),
    Apr. 17, 1953.

17. Seeley, Leonard W.: Flight Investigation of the Position Error
    Associated With Local Air Flow Detectors Installed on a Model
    F9F-2 Aircraft. NAVORD Rep. 2014 (NOTS 646), U. S. Naval Ord.
    Test Station, Inyokern (China Lake, Calif.), Mar. 2, 1953.

18. Hibbs, William H., Allen, Robert B., and Ward, Mary C.: Development
    of a Target-Center Camera and Its Applications in Fire-Control
    Research. NAVORD Rep. 1026 (NOTS 145), U. S. Naval Ordnance Test
    Station (Inyokern, Calif.), Sept. 3, 1948.

19. Keuper, R. F.: Aircraft Angle-of-Attack Determination by Ground
    Photography. NAVORD Rep. 1037 (NOTS 156), U. S. Naval Ord. Test
    Station (Inyokern, Calif.), Sept. 26, 1948.

20. Strand, Otto Neall: A General Method for the Photographic Deter-
    mination of Aircraft Attitude, Angle of Attack, and Related
    Parameters. NAVORD Rep. 3506 (NOTS 1135), U. S. Naval Ord. Test
    Station (China Lake, Calif.), May 26, 1955. (Available from ASTIA
    as AD No. 81135.)

61.2°

17.5°

Vane 0.040" thick

Cone

— 3 1/4" —
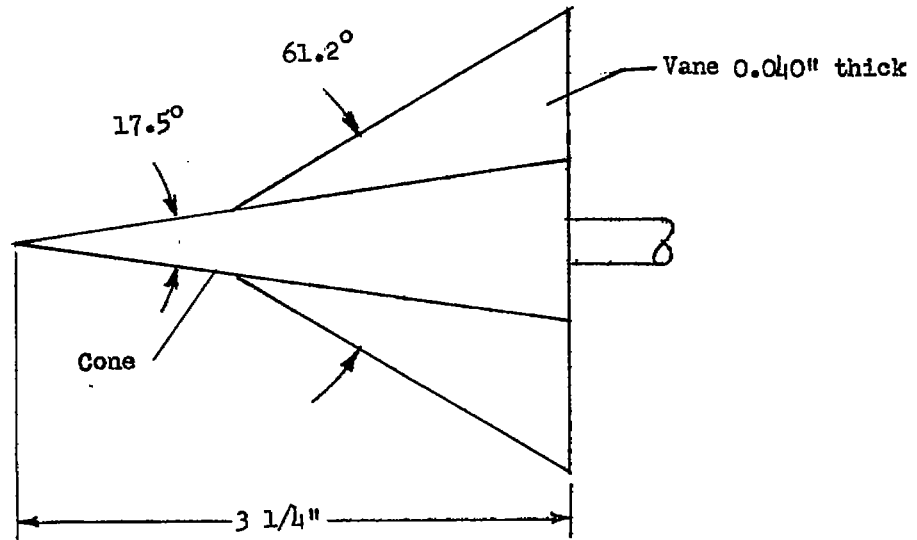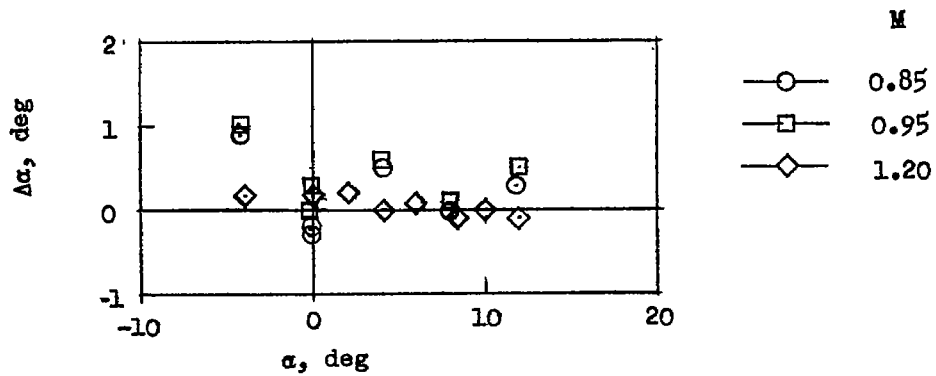
(a) Sensor.

(b) Calibration.

Figure 1.- Calibration of axially mounted pivoted vane at transonic
speeds (ref. 5). β = 0°.
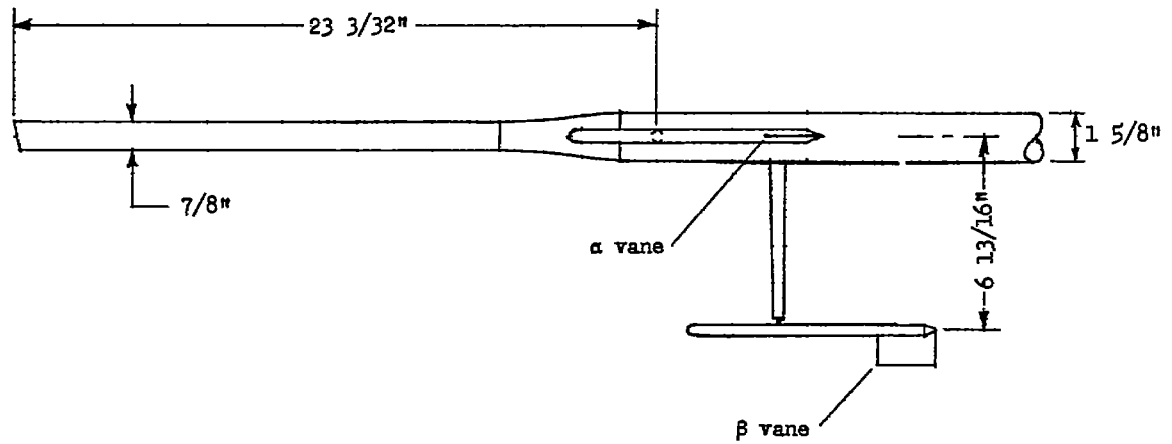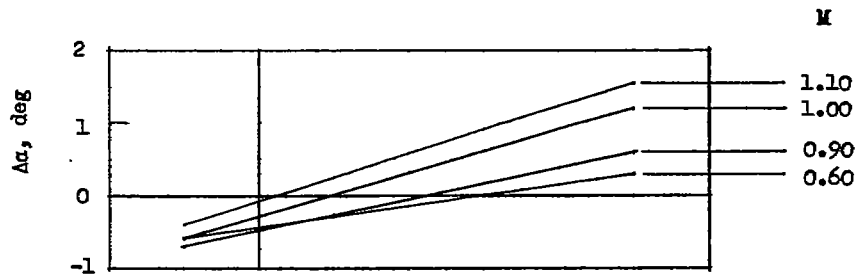
(a) Sensor.

(b) Calibration; transonic (ref. 6).
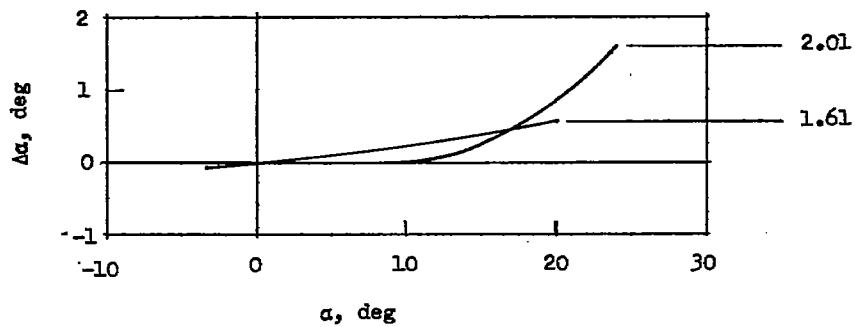
(c) Calibration; supersonic (ref. 7).

Figure 2.- Calibration of transverse-mounted pivoted vane at transonic
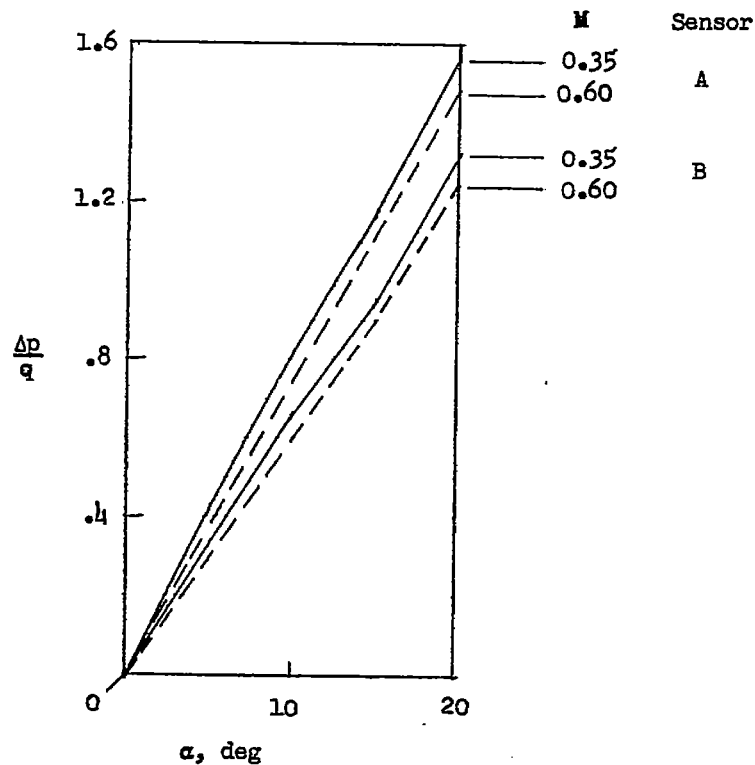and supersonic speeds (refs. 6 and 7). $\beta = 0^{\circ}$.
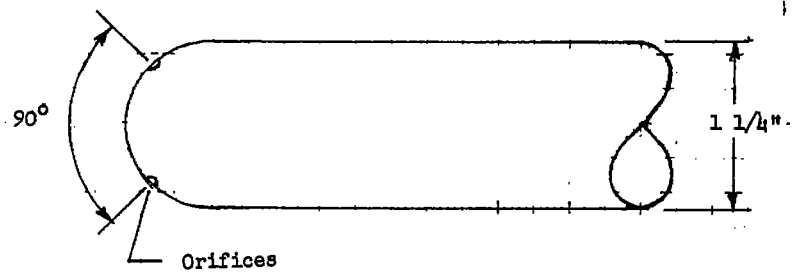
(a) Sensor.
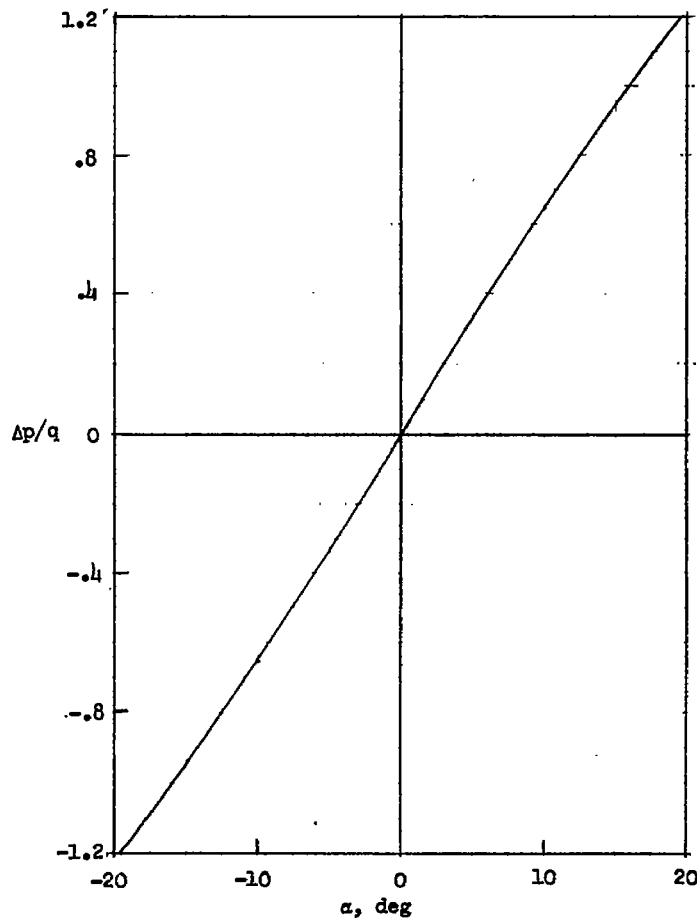
(b) Calibration.

Figure 3.- Variation of $\Delta p/q$ with α of a differential pressure sensor having a hemispherical nose shape from unpublished British tests. $M = 0.11$; $\beta = 0^\circ$.

Sensor A   90°

0.5"

Orifices

Sensor B   60°

Orifices

(a) Sensors.

	M	Sensor
	0.35	A
	0.60	
	0.35	B
	0.60	

$\frac{\Delta p}{q}$

1.6

1.2

.8

.4

0   10   20

α, deg

(b) Calibration.

Figure 4.- Variation of $\Delta p/q$ with α of two differential pressure sensors having hemispherical nose shapes (data from Cornell Aero. Lab., Inc.). $\beta = 0°$.
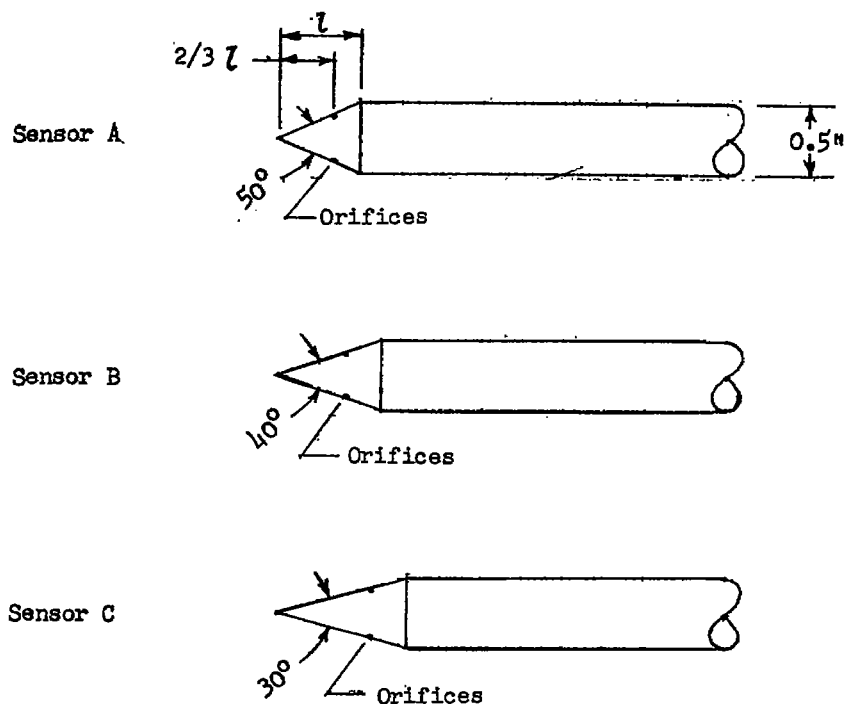
(a) Sensors.
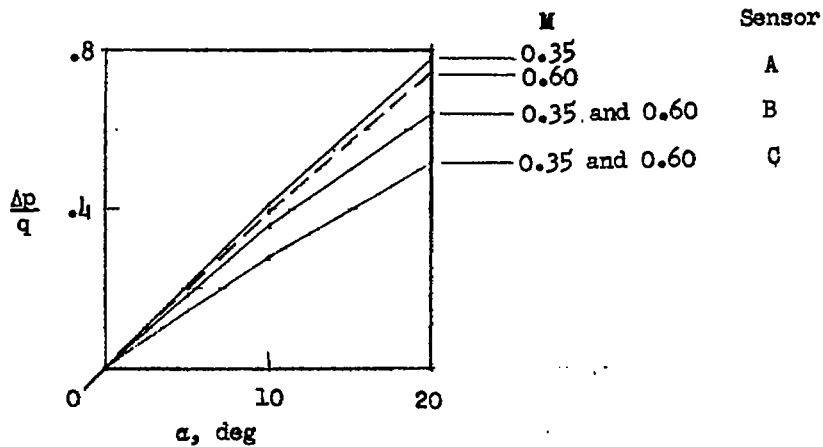
(b) Calibration.

Figure 5.- Variation of $\Delta p/q$ with α of three differential pressure sensors having conical nose shapes. Subsonic speeds (data from Cornell Aero. Lab., Inc.); $\beta = 0°$.
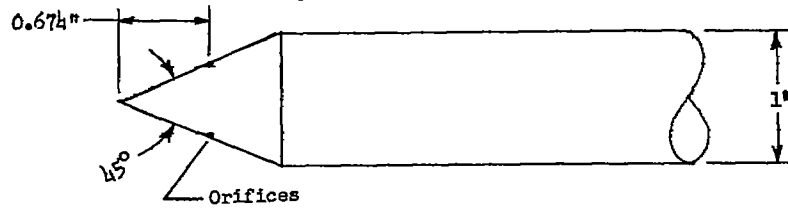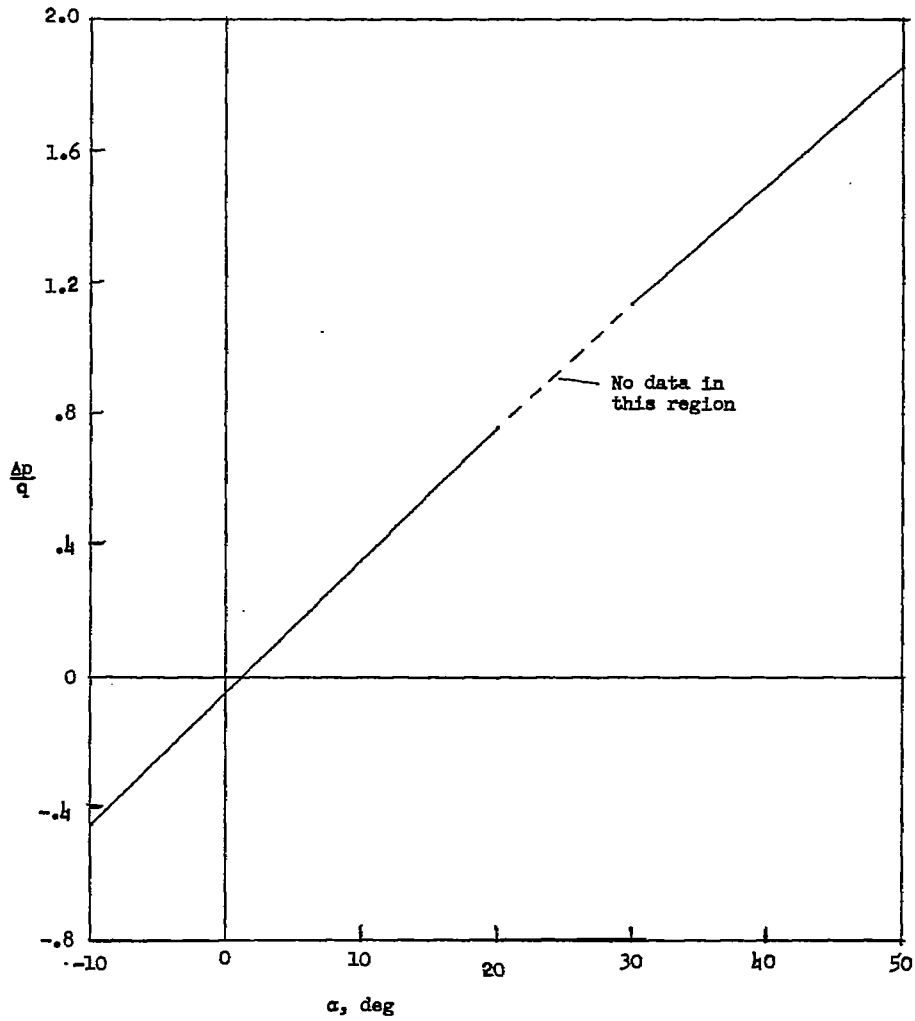
(a) Sensor.

(b) Calibration.

Figure 6.- Variation of $\Delta p/q$ with α of a differential pressure tube having a conical nose shape. M = 0.70 to 1.10 (ref. 10); $\beta = 0^O$.
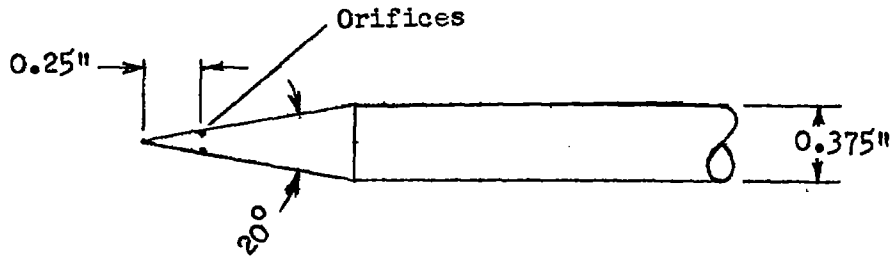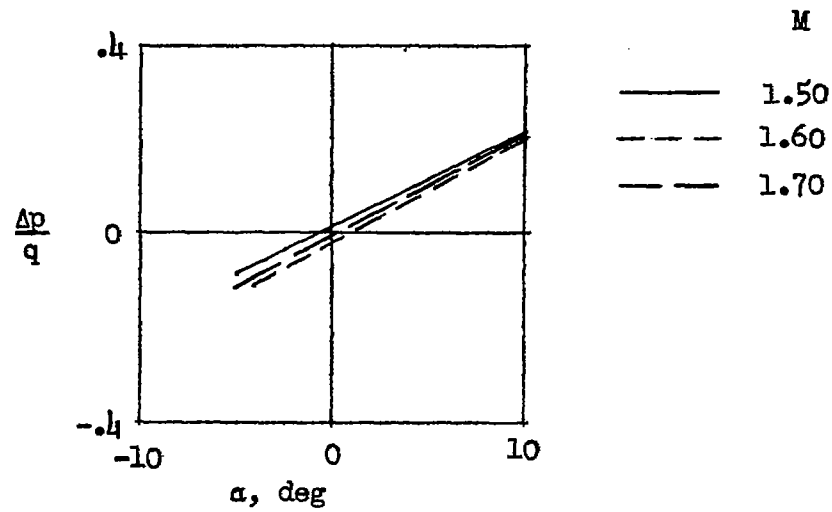
(a) Sensor.

(b) Calibration.

Figure 7.- Variation of $\Delta p/q$ with α of a differential pressure tube having a conical nose shape. Supersonic speeds (ref. 11); $\beta = 0°$.
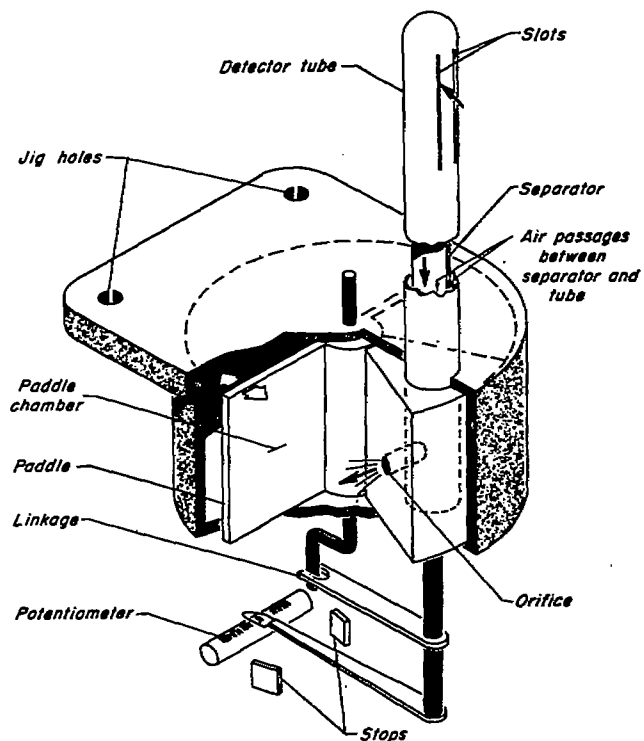
(a) Sensor.
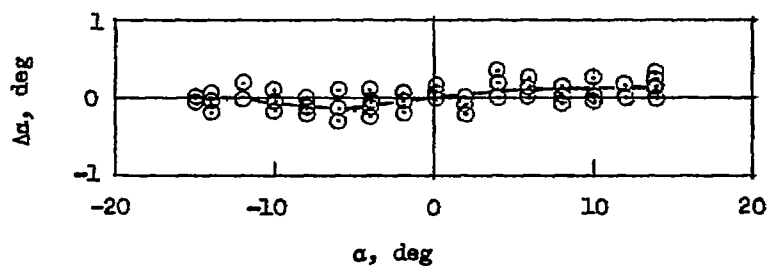
(b) Calibration.

Figure 8.- Calibration of null-seeking pressure-type angle-of-attack
sensor. M = 0.10 (ref. 12); β = 0°.

Axis of rotation

Orifice
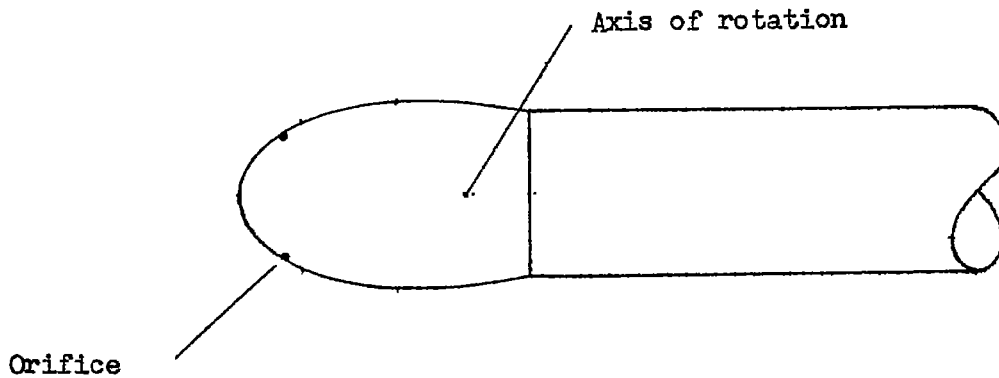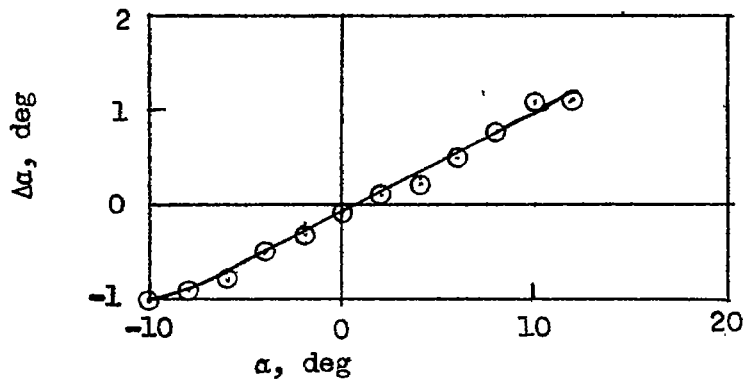
(a) Sensor.

(b) Calibration.

Figure 9.- Calibration of null-seeking pressure-type angle-of-attack
sensor (ref. 8). $\beta = 0^{\circ}$.
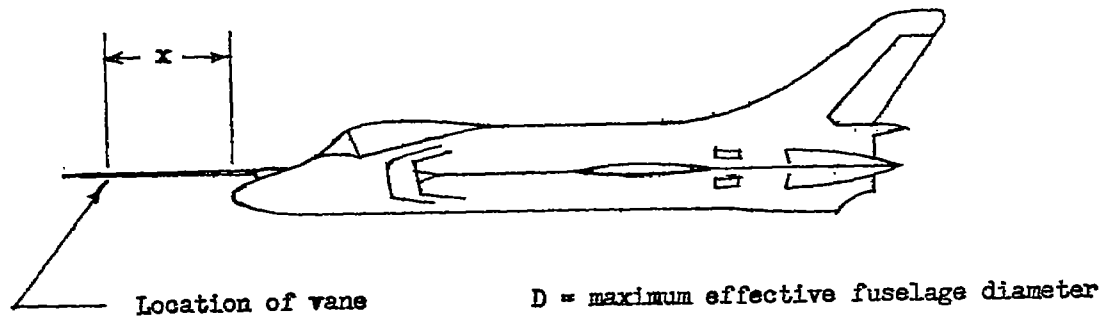
(a) Sensor location on airplane.
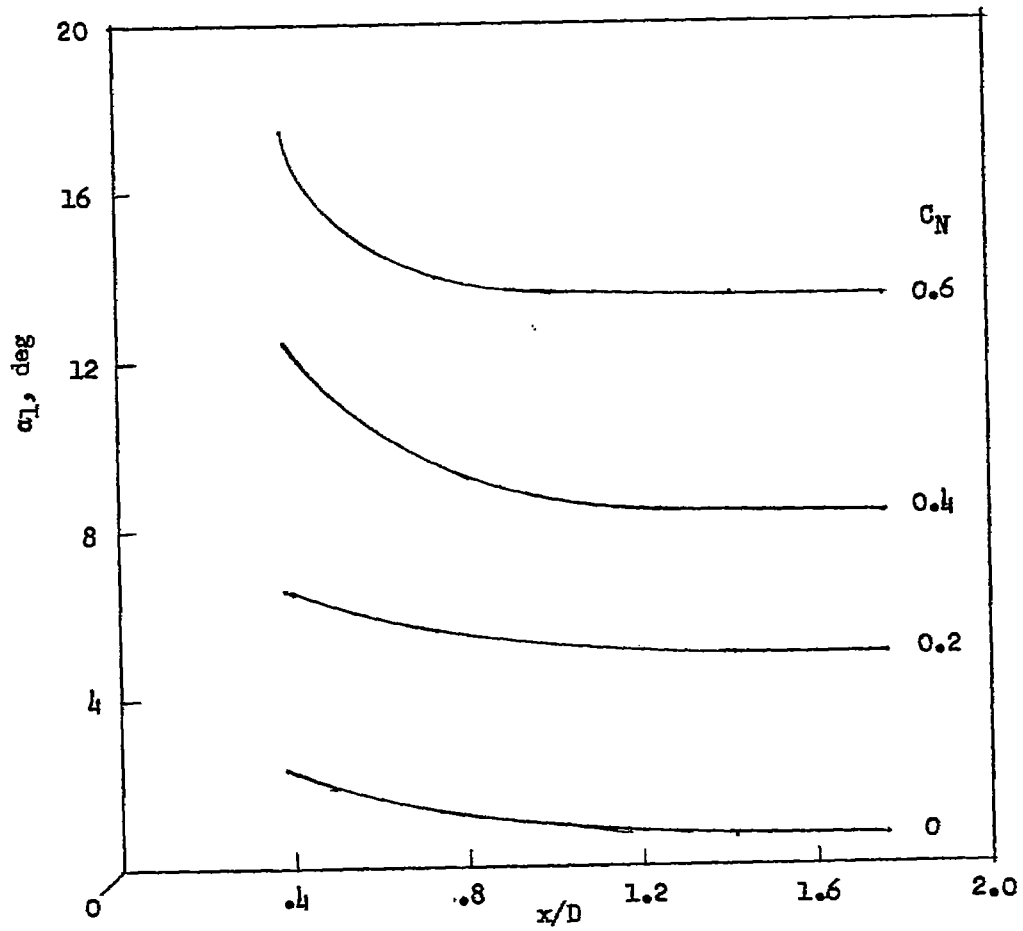
(b) Variation of α_l with x/D.

Figure 10.- Variation of local angle of attack with distance ahead of a fuselage having an ogival nose with rounded tip (data from Ames Aero. Lab.). M = 0.80.
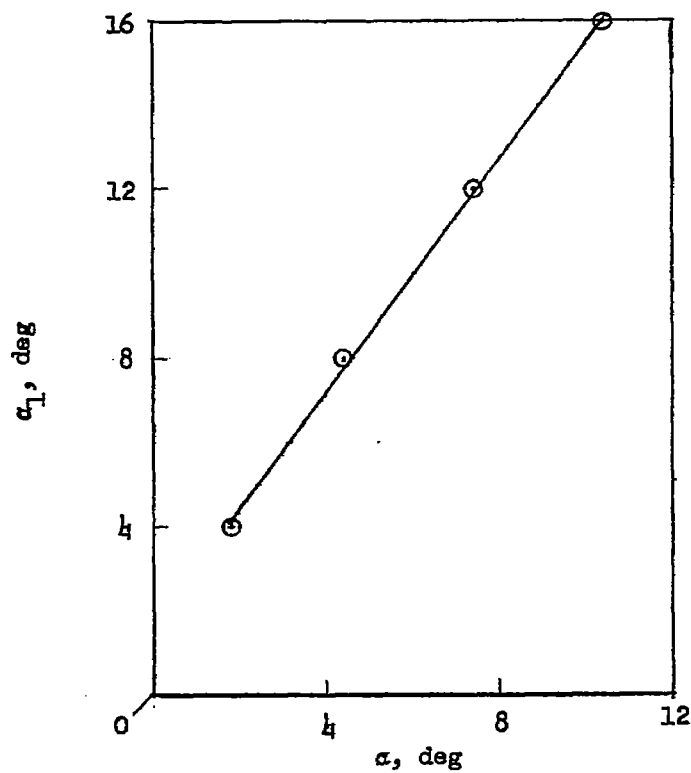
Location of vane   D = maximum effective fuselage diameter
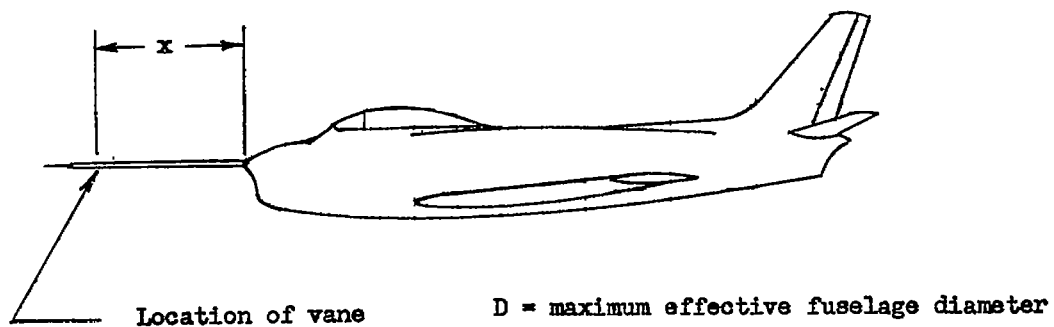
(a) Sensor location on airplane.
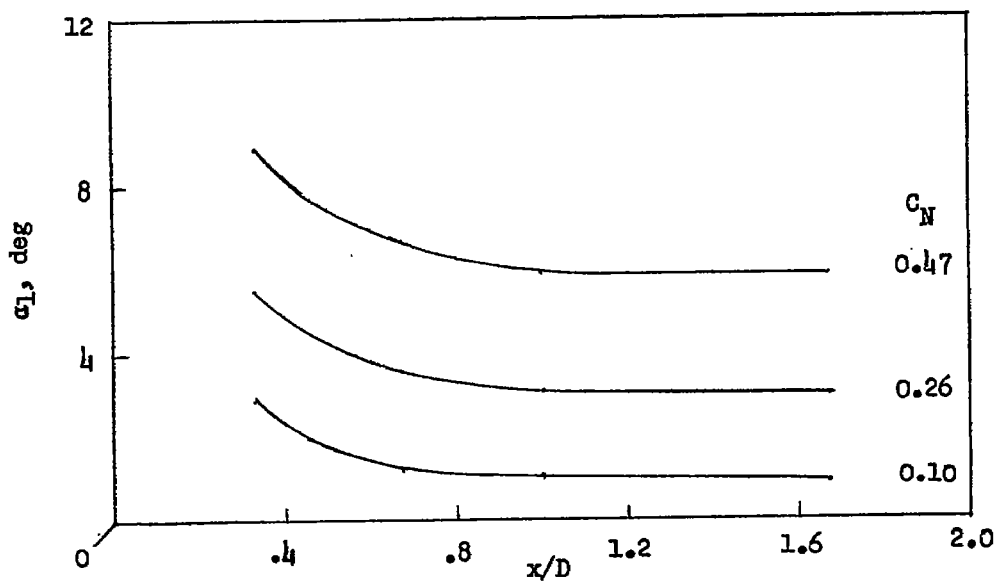
(b) Variation of α_l with x/D.

Figure 11.- Variation of local angle of attack with distance ahead of a
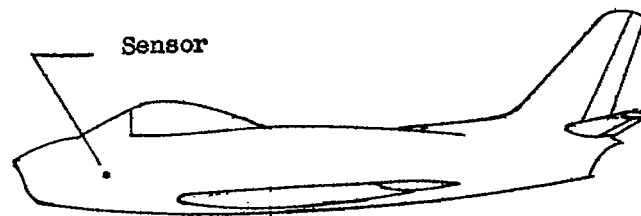fuselage having a nose inlet. M = 0.81 (ref. 13).
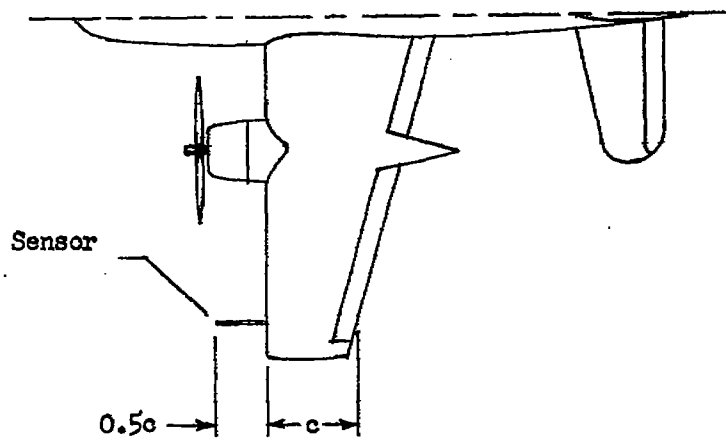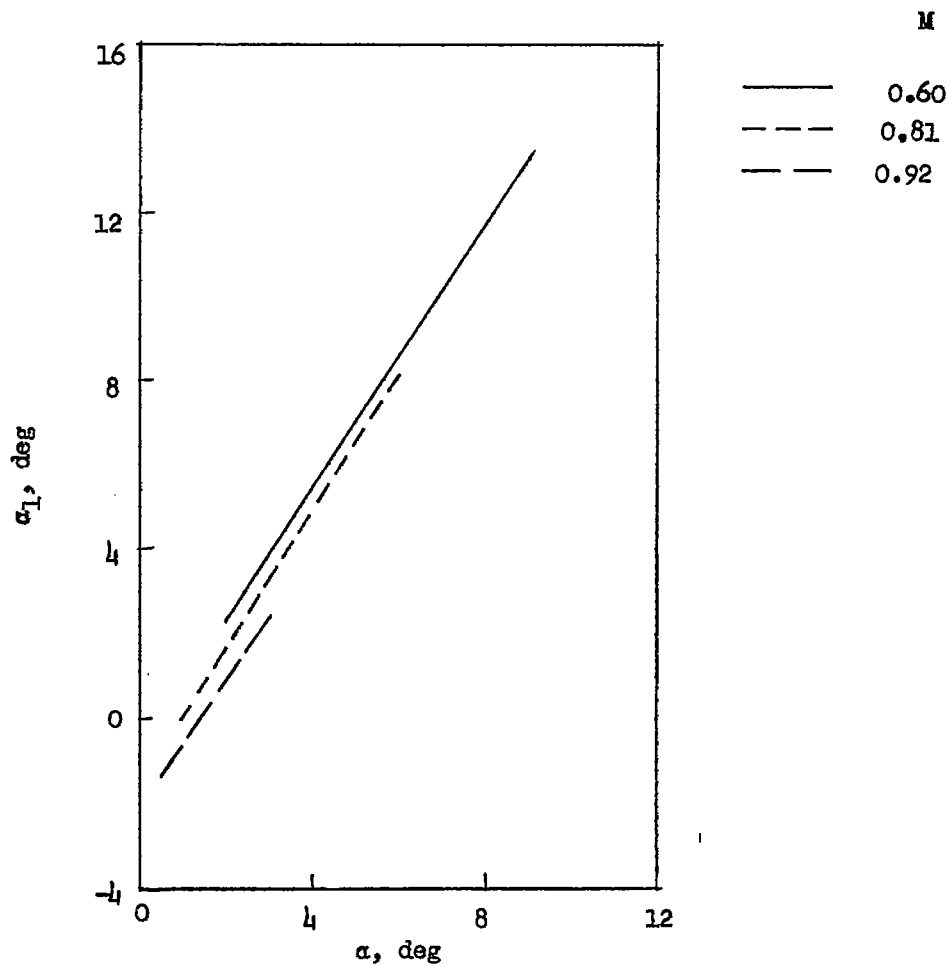
(a) Sensor location on airplane.

(b) Calibration.

Figure 12.- Flight calibration of an angle-of-attack sensor located
    0.5 chord length ahead of the wing tip of an airplane. M = 0.30
    (data from Cornell Aero. Lab., Inc.).

(a) Sensor location on airplane.

(b) Calibration.

Figure 13.- Flight calibration of null-seeking pressure-type angle-of-
attack sensor (of the type shown in fig. 8) installed on the fuse-
lage nose of an airplane (ref. 13).

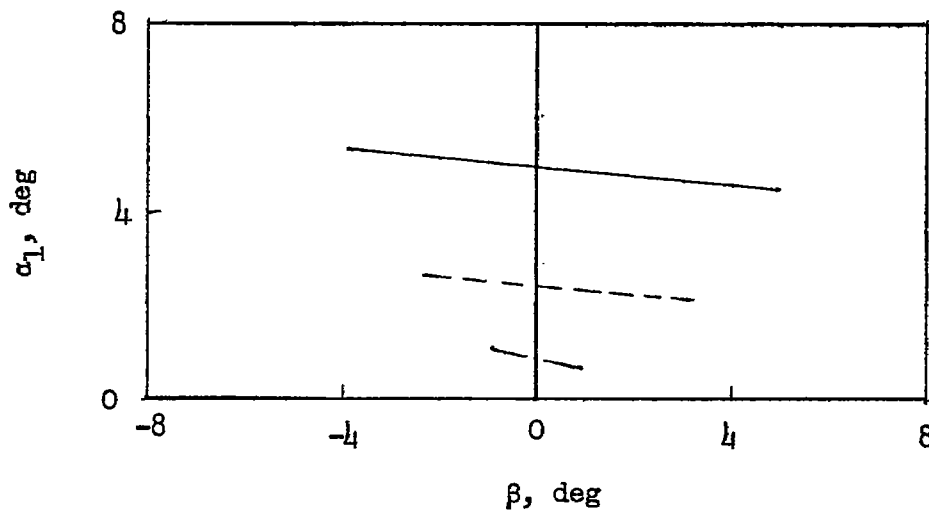|	M	α, deg
————	0.70	3.8
— — —	0.82	2.6
— · —	0.90 and 0.91	2.0

Figure 14.- Effect of sideslip on the angle of attack measured by null-seeking pressure-type sensor (of the type shown in fig. 8) installed on the fuselage nose of an airplane (ref. 13). Installation was the same as that shown in figure 13.